

Stability Analysis of Laminated Cylindrical Shells under Combined Axial Compression and Non-Uniform External Pressure

M. Z. Kabir¹, D. Poorveis²

This study investigates geometrical non-linear analysis of composite circular cylindrical shells under external pressure over part of their surfaces and also shells subjected to combined axial compression and triangular external pressure. Donnell non-linear shell theory along with first order shear deformation theory (FOSD) are adopted in the analysis. In the case of combined axial compression and triangular external pressure post-buckling curves for various shell stacking sequences and different load interaction parameter are traced. Comparison of the results for uniform and triangular external pressures in combination with axial compression applied to the laminated cylindrical shells is carried out in terms of interaction buckling curves as well as load-deflection and load-shortening diagrams.

NOMENCLATURE

A_{ij}	Membrane rigidities	\hat{W}	Initial imperfection function
B_{ij}	Membrane-bending coupling rigidities	$\delta W_{\text{int}}^{sh}$	Internal virtual work
$[C]$	Rigidity matrix	$\delta W_{\text{ext}}^{sh}$	External virtual work
D_{ij}	Bending rigidities	$\epsilon_x, \epsilon_\theta$	Shell mid-surface normal strains
h	Shell thickness	ϕ_x, ϕ_θ	Rotation components
L	Length of cylinder	$\gamma_{x\theta}$	Mid-surface shear strain
m	Longitudinal harmonic	$\gamma_{xz}, \gamma_{\theta z}$	Transverse shear strains
$M_x, M_\theta, M_{x\theta}$	Shell moments	κ_x, κ_θ	Bending curvatures
n	Circumferential harmonic	$\kappa_{x\theta}$	In-plane twist curvature
$N_x, N_\theta, N_{x\theta}$	Shell in-plane forces	ψ	Fiber angle with respect to x-axis
P	Axial compression		
$q(x)$	External pressure		
Q_x, Q_θ	Out of plane shears		
R	Radius of shell mid-surface		
S	Load interaction parameter		
U, V, W	Displacement components		
\bar{U}	Vector of Fourier unknown coefficients		
$\delta U, \delta V, \delta W$	Virtual displacements		

INTRODUCTION

Despite extensive studies on the buckling and post-buckling of laminated composite cylindrical shells subject to axial compression [1-5]; uniform external pressure [6-8]; and combined axial compression and uniform external pressure [9-11]; the application at partial and non-uniform external pressures to the mentioned shells have been less investigated. Xiao and Cheng [12] derived an eight order differential equation to solve the buckling problem of locally loaded orthotropic cylindrical shells. They took into account uniform external pressure applied both on part of the length of the cylinder and, symmetrically, over strips along the generator. The buckling of circular cylindrical

1. *Associa Professor, Department of Civil Engineering, Amirkabir University of Technology, Tehran, Iran*
 2. *Ph.D. Candidate, Department of Civil Engineering, Amirkabir University of Technology, Tehran, Iran*

shells, partially subjected to external liquid pressure, was studied analytically and experimentally by Chiba and his co-workers [13]. Greenberg and Stavsky [14] investigated the static buckling of composite cylinders under circumferentially non-uniform axial loads based on Flugge-type strain-displacement relations.

The current paper explores the stability of composite cylindrical shells under axi-symmetric external pressure applied to the part of their body. Triangular external pressure, as a distinguished distribution, is considered in the analysis. The boundary conditions are assumed to be classically simply supported (SS3). Buckling pressure is calculated by controlling the determinant sign of tangent stiffness matrix. Comparison of the effects of laminate lay-up and external pressure distribution (triangular vs. uniform) on critical pressure is presented by tracing interaction buckling curves. Finally in the case of combined axial compression and triangular pressure, post-buckling curves as uniform end-shortening and radial displacement versus external pressure are plotted.

THEORY

Displacements and rotations are expressed in terms of Fourier series expansions. The equilibrium equations are obtained using the Ritz method. The linearized equations are solved using iterative Newton-Raphson and arc-length methods.

SHELL GEOMETRY

The configuration of shell with global coordinates is sketched in Figure 1. The principal material directions are specified as 1 and 2. The global coordinate system x , θ and z , displacement components U, V, W and rotations ϕ_x and ϕ_θ are also shown in Figure 1. In the same figure, the lateral pressure q , the axial force P , the length L , the thickness h and the radius of curvature of middle surface R are also shown. Ψ is the angle between the principal material axis 1 and the x -axis of the shell.

DISPLACEMENTS AND ROTATIONS

The displacements of an arbitrary point of cylindrical shell is expressed as:

$$\begin{aligned}\bar{U}(x, \theta, z) &= U(x, \theta) + z\phi_x(x, \theta) \\ \bar{V}(x, \theta, z) &= V(x, \theta) + z\phi_\theta(x, \theta) \\ \bar{W}(x, \theta, z) &= W(x, \theta)\end{aligned}\quad (1)$$

where $U(x, \theta)$, $V(x, \theta)$ and $W(x, \theta)$ are displacements of mid-surface of shell in axial, circumferential and radial directions respectively, and $\phi_x(x, \theta)$ and $\phi_\theta(x, \theta)$ are the rotations of normal vector to the surface.

CONSTITUTIVE EQUATIONS

The shell stress-strain relationship is expressed as:

$$\{\sigma\} = [C] \{\epsilon\} \quad (2)$$

where $[C]$ is the generalized material rigidity matrix. The vector of stress resultants is defined as:

$$\{\sigma\} = [N_x, N_\theta, N_{x\theta}, M_x, M_\theta, M_{x\theta}, Q_x, Q_\theta]^T \quad (3)$$

$N_x, N_\theta, N_{x\theta}$ are in-plane forces, $M_x, M_\theta, M_{x\theta}$ represent moments and Q_x, Q_θ are out of plane shear components per unit width. The strain vector $\{\epsilon\}$ is:

$$\{\epsilon\} = [\epsilon_x, \epsilon_\theta, \gamma_{x\theta}, \kappa_x, \kappa_\theta, \kappa_{x\theta}, \gamma_{xz}, \gamma_{\theta z}]^T \quad (4)$$

where $\epsilon_x, \epsilon_\theta$ and $\gamma_{x\theta}$ are mid-surface strains, κ_x and κ_θ are bending curvatures in x - z and θ - z plane, respectively.

$\kappa_{x\theta}$ is in-plane twist curvature and γ_{xz} and $\gamma_{\theta z}$ represent transverse shear strains. $[C]$ matrix is:

$$[C] = \begin{bmatrix} [A] & [B] & o & o \\ [B] & [D] & o & o \\ o & o & A_{44} & o \\ o & o & o & A_{55} \end{bmatrix} \quad (5)$$

A_{ij} , membrane rigidities, B_{ij} , membrane-bending coupling terms, D_{ij} , bending rigidities and transverse shear rigidities A_{44} and A_{55} are defined as:

$$\begin{aligned}(A_{ij}, B_{ij}, D_{ij}) &= \int_h (1, z, z^2) \bar{Q}_{ij} dz \\ A_{44} &= \int_h \bar{Q}_{44} dz, \quad A_{55} = \int_h \bar{Q}_{55} dz\end{aligned}\quad (6)$$

where \bar{Q}_{ij} is transformed reduced stiffness [15].

STRAIN - DISPLACEMENT RELATIONSHIPS

The strains at an arbitrary point of the shell thickness are expressed as follows:

$$e_x = \epsilon_x + z\kappa_x, \quad e_\theta = \epsilon_\theta + z\kappa_\theta, \quad e_{x\theta} = \gamma_{x\theta} + z\kappa_{x\theta} \quad (7)$$

where strains of mid-plane and curvatures based on Donnell and first order shear deformation theories are

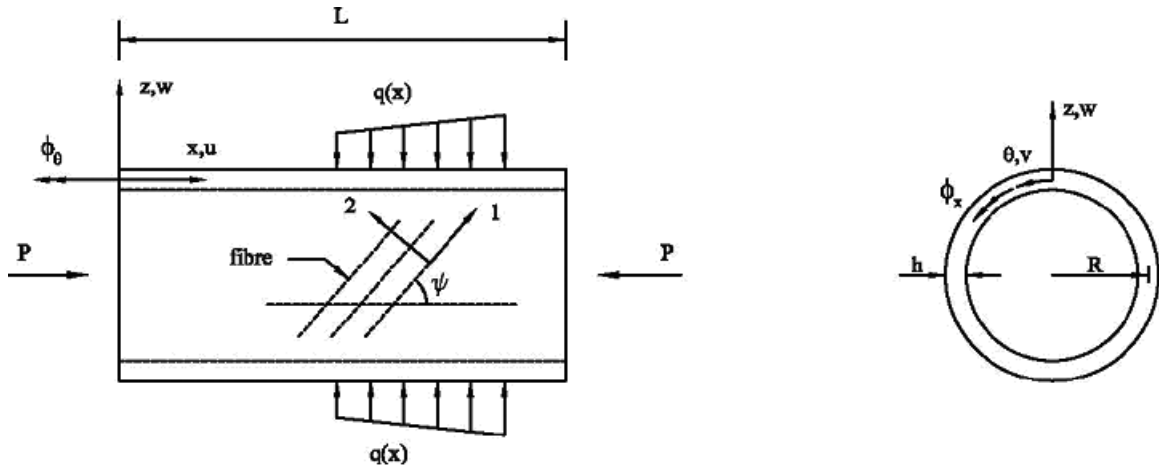


Figure 1. Cylindrical shell with coordinate system, key dimensions and loading, (a) longitudinal view , (b) circumferential view.

as follows:

$$\begin{aligned}
 \epsilon_x &= \frac{\partial U}{\partial x} + \frac{1}{2} \left(\frac{\partial W}{\partial x} \right)^2 + \left(\frac{\partial \hat{W}}{\partial x} \right) \left(\frac{\partial W}{\partial x} \right) \\
 \epsilon_\theta &= \frac{1}{R} \frac{\partial V}{\partial \theta} + \frac{W}{R} + \frac{1}{2R^2} \left(\frac{\partial W}{\partial \theta} \right)^2 + \frac{1}{R^2} \left(\frac{\partial \hat{W}}{\partial \theta} \right) \left(\frac{\partial W}{\partial \theta} \right) \\
 \gamma_{x\theta} &= \frac{1}{R} \frac{\partial U}{\partial \theta} + \frac{\partial V}{\partial x} + \frac{1}{R} \left(\frac{\partial W}{\partial x} \right) \left(\frac{\partial W}{\partial \theta} \right) \\
 &\quad + \frac{1}{R} \left(\frac{\partial W}{\partial x} \right) \left(\frac{\partial \hat{W}}{\partial \theta} \right) + \frac{1}{R} \left(\frac{\partial \hat{W}}{\partial x} \right) \left(\frac{\partial W}{\partial \theta} \right) \\
 \kappa_x &= \frac{\partial \phi_x}{\partial x}, \quad \kappa_\theta = \frac{1}{R} \frac{\partial \phi_\theta}{\partial \theta}, \quad \kappa_{x\theta} = \frac{1}{R} \frac{\partial \phi_x}{\partial \theta} + \frac{\partial \phi_\theta}{\partial x} \\
 \gamma_{xz} &= \phi_x + \frac{\partial W}{\partial x}, \quad \gamma_{\theta z} = \phi_\theta + \frac{1}{R} \left(\frac{\partial W}{\partial \theta} \right)
 \end{aligned} \quad (8)$$

\hat{W} is initial imperfection in the form of buckling mode. Due to the use of the Donnell-type non-linear kinematics relations, the analysis is restricted to

shallow shells. For simply supported end conditions, the double expansions of Fourier series are:

$$\begin{aligned}
 U(x, \theta) &= (x - L/2)U_{x0} + \sum_{m=1}^M \sum_{n=0}^N U_{mn} \text{Cos}(\alpha_m x) \text{Cos}(n\theta) \\
 V(x, \theta) &= \sum_{m=1}^M \sum_{n=1}^N V_{mn} \text{Sin}(\alpha_m x) \text{Sin}(n\theta) \\
 W(x, \theta) &= \sum_{m=1}^M \sum_{n=0}^N W_{mn} \text{Sin}(\alpha_m x) \text{Cos}(n\theta) \\
 \phi_x(x, \theta) &= \sum_{m=1}^M \sum_{n=0}^N \phi_{mn} \text{Cos}(\alpha_m x) \text{Cos}(n\theta) \\
 \phi_\theta(x, \theta) &= \sum_{m=1}^M \sum_{n=1}^N \phi_{\theta mn} \text{Sin}(\alpha_m x) \text{Sin}(n\theta)
 \end{aligned} \quad (9)$$

in which $\alpha_m = m\pi/L$ and M and N are the upper limit of integer numbers m and n. The unknown coefficients

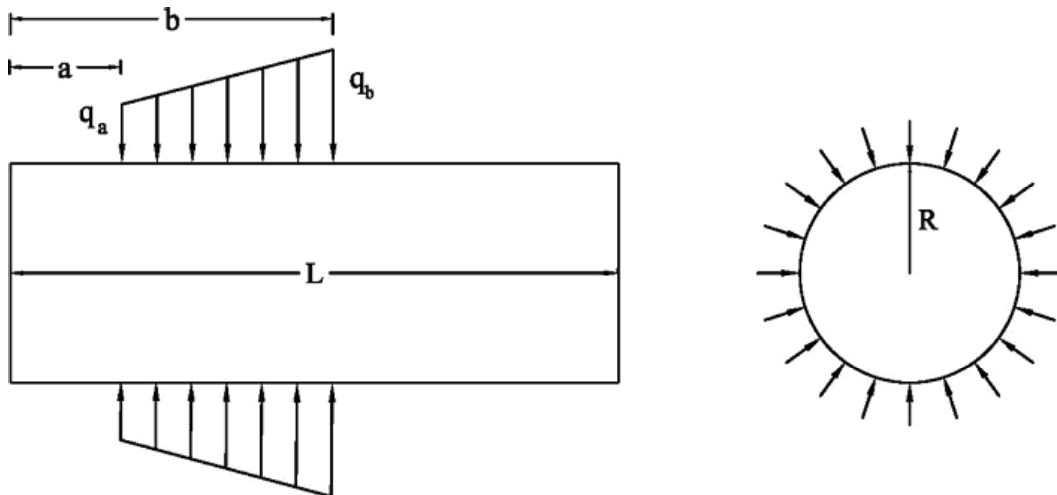


Figure 2. Circular cylindrical shell subjected to linearly varying axisymmetric external pressure over part of its length, (a) longitudinal profile , (b) circumferential view.

U_{x0} , U_{mn} , V_{mn} , W_{mn} , ϕ_{xmn} and $\phi_{\theta mn}$ are modified in each incremental step.

NON-LINEAR ANALYSIS

The total virtual work of cylinder is obtained by combining internal virtual work of shell and external virtual work due to applied loads. The internal virtual work of cylindrical shell is:

$$\begin{aligned} \delta W_{int}^{sh} = & \iint_S [N_x \delta \epsilon_x + N_\theta \delta \epsilon_\theta + N_{x\theta} \delta \gamma_{x\theta} + M_x \delta \kappa_x \\ & + M_\theta \delta \kappa_\theta + M_{x\theta} \delta \kappa_{x\theta} + Q_x \delta \gamma_{xz} + Q_\theta \delta \gamma_{\theta z}] dS \end{aligned} \quad (10)$$

The external virtual work due to axial and lateral applied pressure is:

$$\delta W_{ext}^{sh} = -P \int_0^{2\pi} [\delta U(l, \theta) - \delta U(0, \theta)] R d\theta - q^D \int_S \delta W dS \quad (11)$$

in which P is the axial force per unit length of cylinder circumference and q^D is the radial dead pressure. For hydrostatic pressure, P is related to q^D ($P = Rq^D/2$). In the case of live external pressure, which is displacement dependent [16], the second term of equation (11) is modified as:

$$\begin{aligned} -q^L \int_S [\delta W + \frac{1}{R}(V\delta V + W\delta W) + \delta W(\frac{\partial U}{\partial x} + \frac{1}{R}\frac{\partial V}{\partial \theta}) \\ + W(\frac{\partial \delta U}{\partial x} + \frac{1}{R}\frac{\partial \delta V}{\partial \theta})] dS \end{aligned} \quad (12)$$

The equilibrium equations are in the form of:

$$\delta W_{total}^{sh} = \delta W_{int}^{sh} - \delta W_{ext}^{sh} = 0 \quad (13)$$

After linearization of Eq. (13), the incremental equilibrium equations can be written as:

$$\delta W_{total}^{sh}(\bar{U}) + D\delta W_{total}^{sh}(\bar{U})[\Delta\bar{U}] = 0 \quad (14)$$

where $D\delta W_{total}^{sh}(\bar{U})[\Delta\bar{U}]$ represents directional derivative of total virtual work at \bar{U} in the direction of $\Delta\bar{U}$ [17]. It is to be noted that vector \bar{U} stores Fourier unknown coefficients and $\Delta\bar{U}$ is its increment. Equation (14) is fundamental relation for non-linear analysis in Newton-Raphson and arc-length methods [18].

NON-UNIFORM EXTERNAL PRESSURE

A linearly varying axisymmetric external pressure applied to the partial segment of the shell is shown in

Figure 2. External virtual work due to the dead form of this loading is defined as:

$$W_{ext}^q = \int_0^{2\pi} \int_0^L q(x) \delta W(x, \theta) R dx d\theta \quad (15)$$

in which $q(x)$ is pressure at a distance x , and $\delta W(x, \theta)$ represents virtual radial displacement at coordinate (x, θ) . Substituting $q(x) = q_a + \frac{(q_b - q_a)}{(b-a)}(x - a)$ and $\delta W(x, \theta)$ in equation (15) leads to:

$$\begin{aligned} \delta W_{ext}^q = & - \frac{2RL}{(b-a)} [q_b(a+b) - 2q_a b] \sum_{m=1,2,\dots}^M \frac{1}{m} \cos \frac{m\pi b}{L} \delta W_{m0} \\ & - \frac{2RL}{(b-a)} [q_a(a+b) - 2q_b a] \sum_{m=1,2,\dots}^M \frac{1}{m} \cos \frac{m\pi a}{L} \delta W_{m0} \\ & - \frac{2RL^2}{(b-a)} (q_b - q_a) \sum_{m=1,2,\dots}^M \frac{1}{m^2} (\sin \frac{m\pi b}{L} - \sin \frac{m\pi a}{L}) \delta W_{m0} \end{aligned} \quad (16)$$

where δW_{m0} is axisymmetric virtual radial displacement for harmonic m . External virtual work due to the live type (displacement dependent) of partial loading can be obtained by adding the expanded form of equation (12) to relation (16).

NUMERICAL RESULTS AND DISCUSSIONS

A computer program based on the described analysis is prepared to assess the stability of composite cylindrical shells under longitudinally partial and non-uniform external pressure. For the uniform partial loading with variable loaded length, a numerical example from Reference [12] for comparing the results is analyzed. Another set of studies is carried out to compare buckling and post-buckling response of various laminated cylindrical shells subject to combined axial compression and triangular external pressure with those of axial compression in combination with uniform external pressure.

CYLINDER UNDER PARTIAL EXTERNAL PRESSURE

Figure 3a shows axisymmetric uniform partial pressure. In an attempt to validate the current analysis, the buckling of composite cylinders under partial external pressure is investigated. The present results are compared with those given by Xiao and Cheng [12]. Geometry of the cylinder according to Figure 1 is as follows: $L/R=5$; $h/R=0.01$ and $R=128.0$ mm. Also, material properties include two cases: isotropic material with $\nu = 0.0165$ and orthotropic material

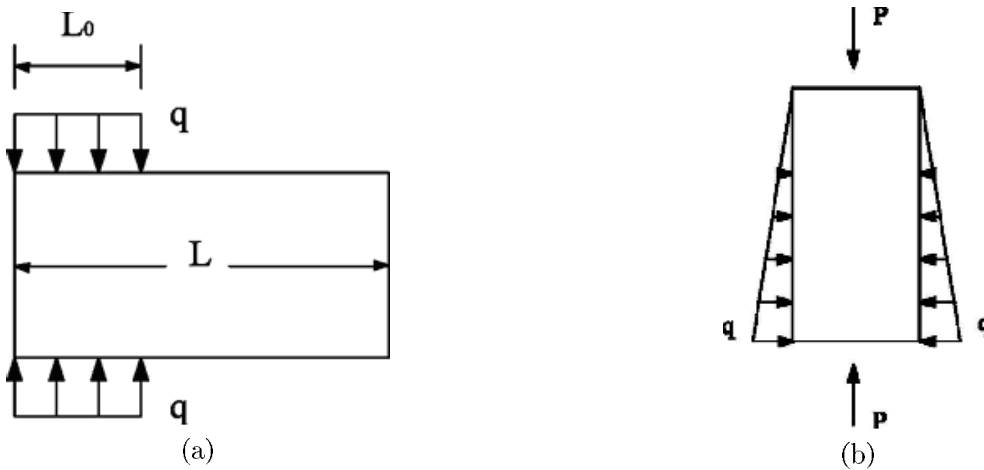


Figure 3. Cylindrical shell subjected to axisymmetric partial loading, (a) uniform partial loading, (b) combined axial compression and triangular lateral pressure.

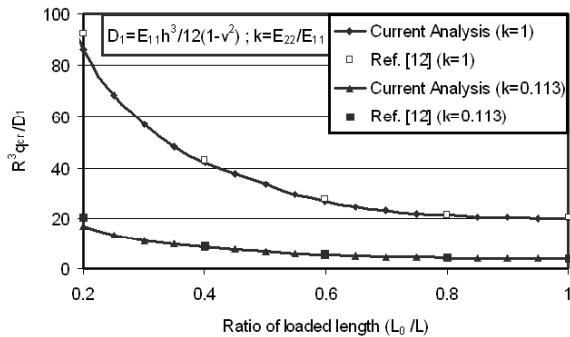


Figure 4. Buckling of orthotropic circular cylinder under partial uniform external pressure.

with $k = E_{22} / E_{11} = 0.113$; $G_{12} / E_{11} = 0.16$; $\nu_{12} = 0.0165$. The ratio of L_0 / L , which represents the loaded area, varies from 0.2 to 1.0. The analytical Results based on geometrical non-linear analysis including pre-buckling deformations are depicted in Figure 4. In each category (isotropic or orthotropic cylinder) 5 discrete square points show those obtained by Reference [12]. For $L_0 / L > 0.4$, the current results are in good agreement with those of Reference [12] for both isotropic and orthotropic material properties. However, for $L_0 / L = 0.2$, some variations exist between the results. For a small ratio of loaded length, pre-buckling deformations take the bending pattern rather than the membrane one, and this domination which has not been included in the investigations by Xiao and Cheng, is the main reason for discrepancies.

COMPOSITE CYLINDER UNDER COMBINED LOADING

The intention of designing this numerical example is to appraise the effects of two types of combined loading on the buckling and post-buckling responses of composite cylindrical shells. The first type is combined axial

compression and triangular external pressure (Figure 3b), and the second loading is uniform external pressure (applied over entire circumference of the cylinder) in combination with axial compression. Several load interaction parameters, S , defined by: $P = SqR$ where (P is axial load per unit length of the circumference and q is the external pressure) along with various shell arrangements, $(90)_4$, $(0/90)_{2T}$, $(75/-75)_{2T}$ are considered in the analyses. The geometric data of the cylinder is: $L = 300.0$ mm; $R = 191.0$ mm; $h = 1.0$ mm; all plies of the skin are of equal thickness and the material properties of one ply is: $E_{11} = 150.0$ GPa; $E_{22} = 7.0$ GPa; $G_{12} = 3.5$ GPa; $\nu_{12} = 0.3$.

Uniform and triangular interaction buckling curves for shell lay-up $(0/90)_{2T}$ are depicted in Figure 5a. Similar curves for other shell arrangements, $(75/-75)_{2T}$ and $(90)_4$, are also shown in Figures 5b and 5c, respectively. The stable region for lay-up $(75/-75)_{2T}$ is partly different from those of $(90)_4$ and $(0/90)_{2T}$ for both uniform and triangular pressures. Another comparison shows that in the case of $(75/-75)_{2T}$ both triangular and uniform interaction buckling diagrams are nearly the same while for $(0/90)_{2T}$ that of uniform pressure encounters more stable behavior and for lay-up $(90)_4$ this trend is the reverse.

Figures 6 and 7 show, respectively, the post-buckling load-shortening and load-deflection curves of various composite cylinders under combined loading. Load interaction parameter, S , is taken 0.5 which corresponds to cylinder under hydrostatic external pressure. For both uniform and triangular pressures, laminated shells with stacking sequences of $(0/90)_{2T}$ and $(75/-75)_{2T}$ have specific minimum strength in the post-buckling domain while that of lay-up $(90)_4$ has a descending pattern in the post-buckling region. In all cases of uniform pressure, the increase in the post-buckling applied pressure causes an increase in the end-

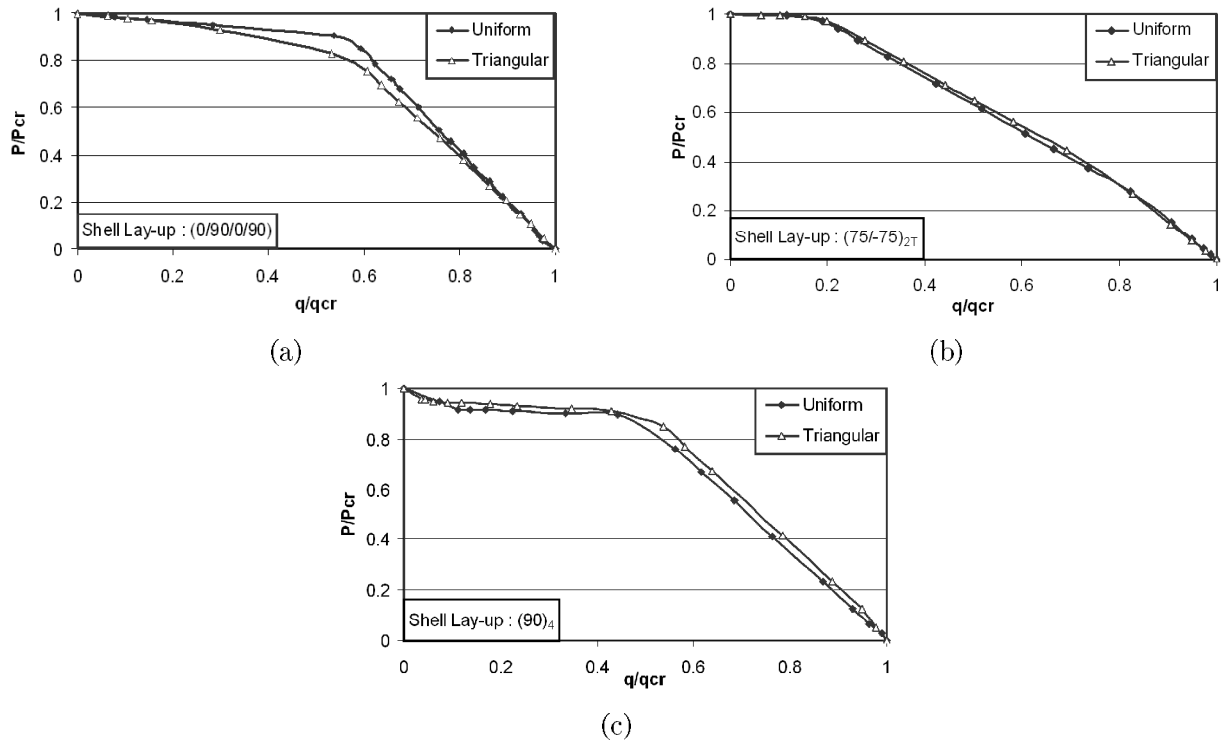


Figure 5. Comparison of buckling interaction curves for uniform and triangular external pressure for various shell arrangements, (a) $(0/90)_{2T}$, (b) $(75/-75)_{2T}$, (c) $(90)_4$.

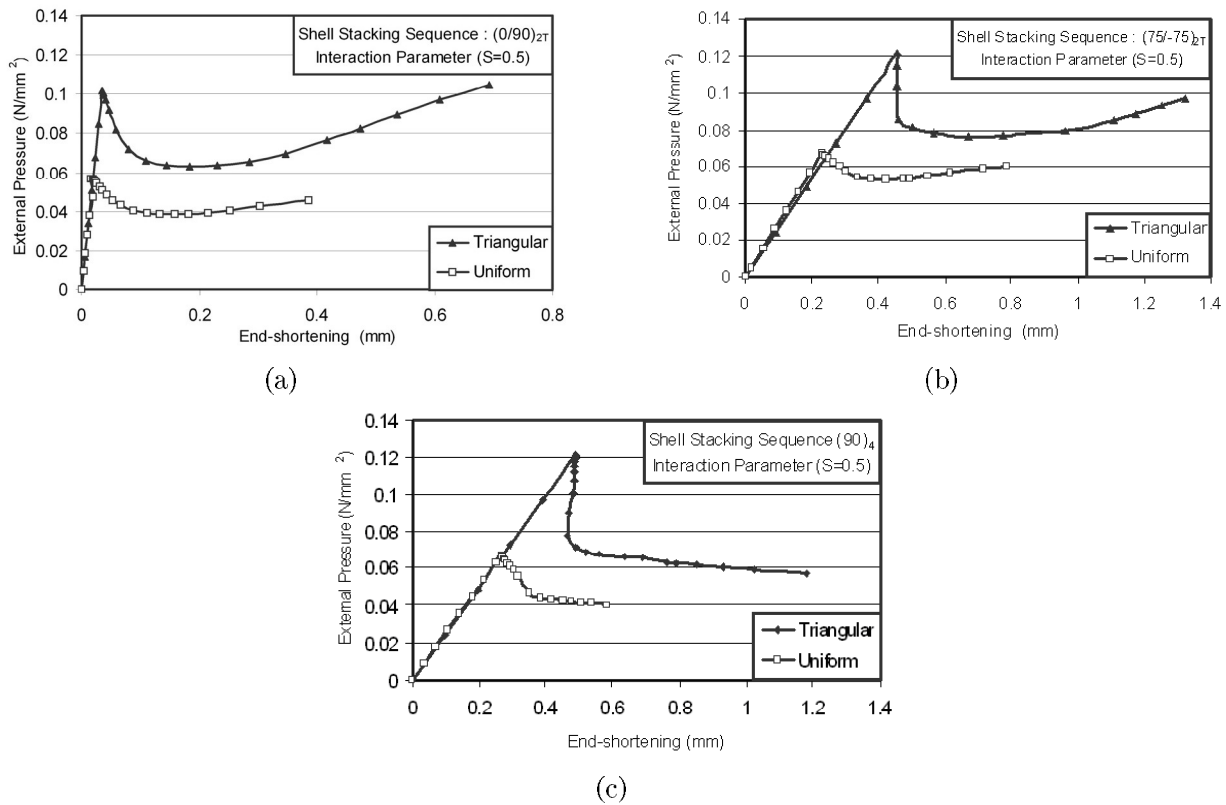


Figure 6. The effect of external pressure distribution on the post-buckling response of a composite cylinder based on end-shortening curves, (a) $(0/90)_{2T}$, (b) $(75/-75)_{2T}$, (c) $(90)_4$.

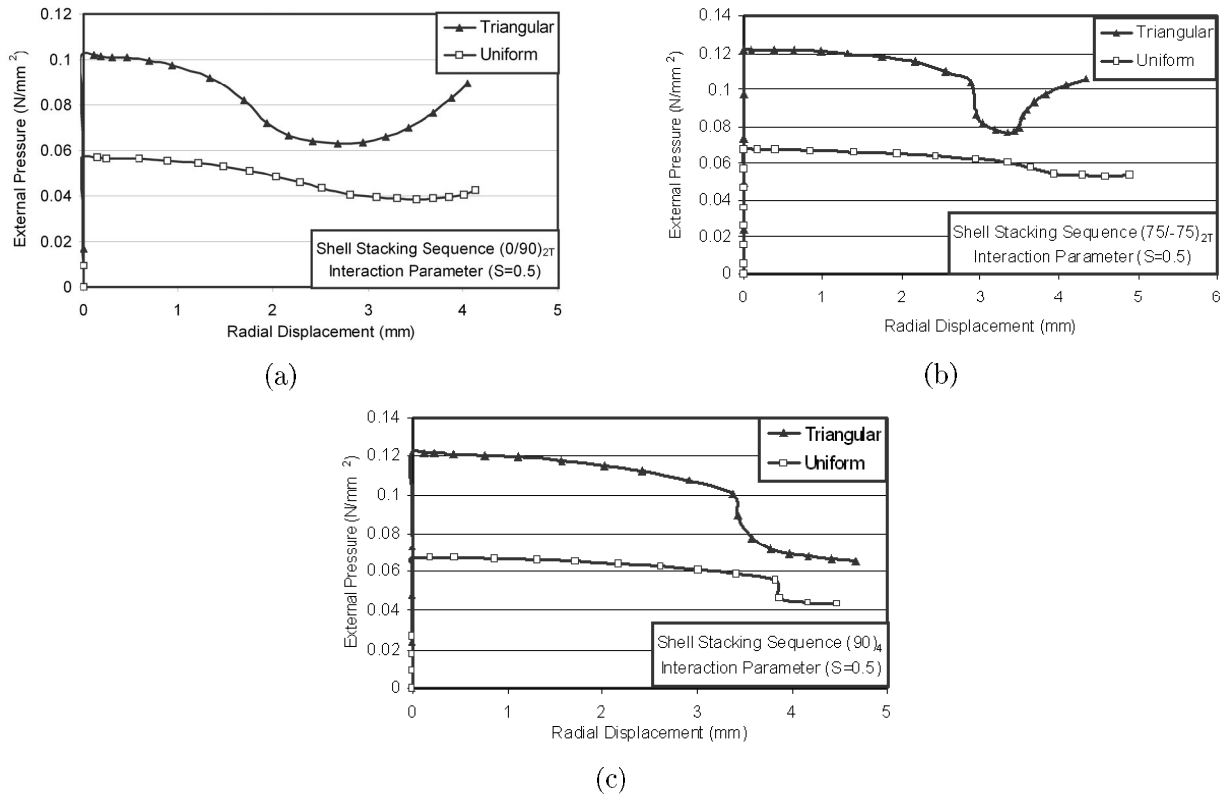


Figure 7. The effect of external pressure distribution on post-buckling response of a composite cylinder based on radial displacement curves, (a) $(0/90)_{2T}$, (b) $(75/-75)_{2T}$, (c) $(90)_4$.

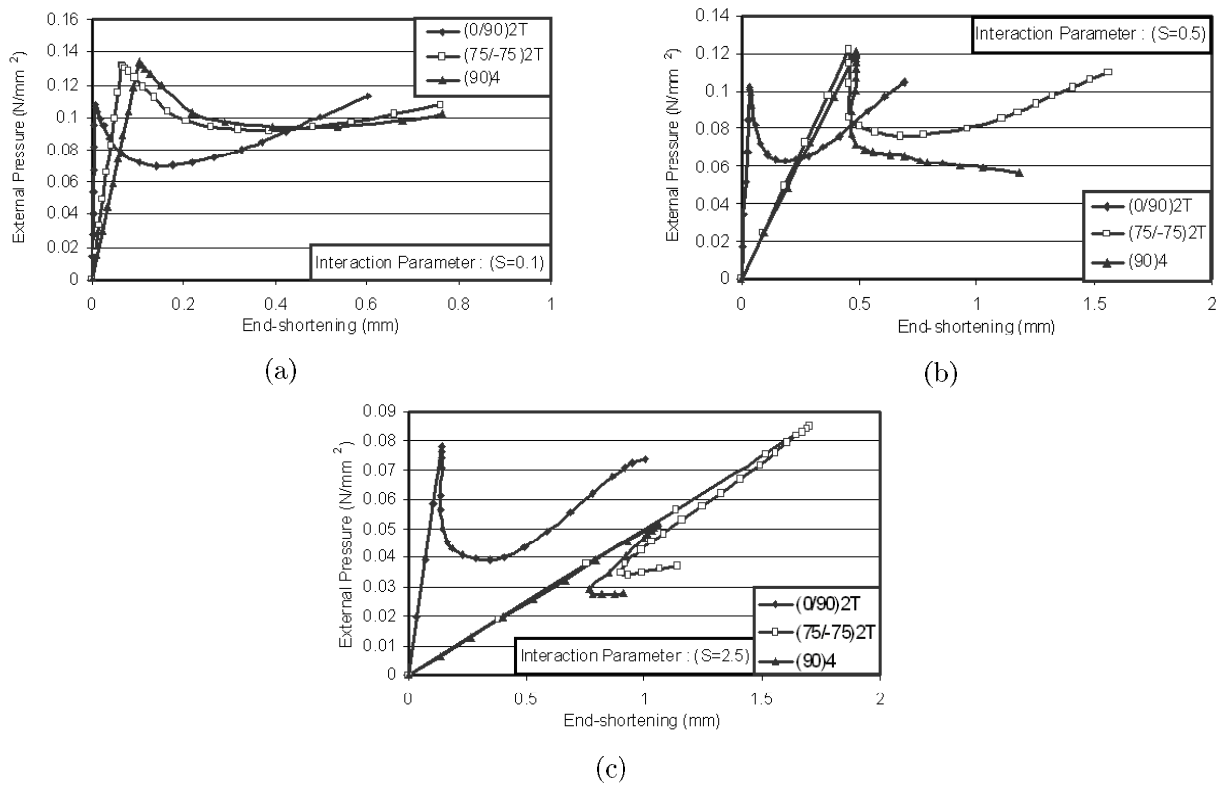


Figure 8. Stacking sequence effects on the post-buckling response of a composite cylinder under combined axial compression and triangular external pressure, (a) $S=0.1$, (b) $S=0.5$, (c) $S=2.5$.

shortening, however, in the case of triangular pressure, there is a slight snap-back in the post-buckling area. Another parameter, which can appraise the post-buckling response, is the ratio of P_{min}/P_{cr} (P_{min} is the lowest post-buckling load). In the case of $(0/90)_{2T}$, P_{min}/P_{cr} is 0.619 for triangular and 0.680 for uniform pressure while $(75/-75)_{2T}$ shows 0.627 and 0.790 for triangular and uniform cases respectively. In the case of triangular external pressure and in the last portion of the post-buckling curves, increase in the strength for shell lay-ups $(0/90)_{2T}$ and $(75/-75)_{2T}$ is identified. However, for uniform pressure case, apart from shell arrangement, stable post-buckling region is negligible.

Figure 8 illustrates the response of different composite cylindrical shells under combined axial compression and triangular external pressure. In this case load interaction parameter, S , varies from 0.1 (nearly pure external pressure) to 2.5 (dominating axial compression). Results show that increasing the S intensifies the snap-back pattern of post-buckling curves for all shell profiles. Also, P_{min}/P_{cr} decreases when increasing the S . In the case of low axial compression ($S=0.1$), despite differences in the critical pressures of the shell made up of various lay-ups, their post-buckling responses are similar. But by increasing the axial compression, relative to the external pressure behavior of post-buckling the response for a shell with $(75/-75)_{2T}$ and $(90)_4$ varies more rapidly than that of $(0/90)_{2T}$.

CONCLUSION

Geometrical non-linear analysis is implemented to study the buckling and post-buckling responses of laminated circular cylindrical shells subjected to combined axial compression and non-uniform external pressure. The Donnell non-linear shell theory along with first order shear deformation (FOSD) is used. The remarkable conclusions based on the obtained information may be classified as follows:

- Comparison of the current study for isotropic and orthotropic cylinders under partial uniform external pressure with those of linear bifurcation analysis indicates that for small loaded portions, pre-buckling bending deformations play a significant role in determining the buckling pressure.
- Interactive buckling curves obtained under combined axial compression and external pressure show that distribution of external pressure (triangular vs. uniform) only has a negligible effect on the pattern and stable zone of these curves. However, the shell stacking sequence has more influence on the shape of interaction buckling curves.
- The post-buckling response of laminated cylindrical shells under combined loading is more sensitive to axial compression than external pressure. Lam-

inated composite cylinders subject to triangular external pressure combined with axial compression show slightly more sensitivity and reduction of the strength in the post-buckling range than those of uniform pressure in combined axial load.

- The shell stacking sequence and load interaction parameter S , both influence post-buckling pattern under combined loading. If these effects intensify each other, snap-backing may occur as in the case of anti-symmetric angle ply laminate, $(75/-75)_{2T}$.

REFERENCES

1. Jun, S. M. and Hong, C. S., "Buckling behaviour of laminated composite cylindrical panels under axial compression", *Comput. & Struct.*, **29**(3), PP 479-490(1988).
2. Soldatos, K. P., "Buckling of shear deformable antisymmetric angle-Ply laminated cylindrical panels under axial compression", *J. of Press. Vess. Tech.*, PP 353-357(1992).
3. Kardomateas, G. A., "Stability loss in thick transversely isotropic cylindrical shell under axial compression", *J. of Appl. Mech.*, PP 506-513(1993).
4. Kardomateas, G. A., "Bifurcation of equilibrium in thick orthotropic cylindrical shell under axial compression", *J. of Appl. Mech.*, PP 43-52(1995).
5. Li, Y. W., Elishakoff, I. and Starnes, J. H. Jr., "Axial buckling of composite cylindrical shell with periodic thickness variation", *Comput. & Struct.*, **56**(1), PP 65-74(1995).
6. Shen, H. S. and Chen, T. Y., "A boundary layer theory for the buckling of thin cylindrical shells under external pressure", *Appl. Math. Mech.*, **9**, PP 557-571(1988).
7. Yang, J. L., Zhang, Y. and Zhang, Z. M., "Non-linear stability analysis of infinitely long laminated cylindrical shallow shells including shear deformation under lateral pressure", *Int. J. Mech. Sci.*, **34**(5), PP 345-354(1992).
8. Kardomateas, G. A., "Buckling of thick orthotropic cylindrical shells under external pressure", *J. of Appl. Mech.*, **60**, PP 195-202(1993).
9. Sun, G. and Hansen, J. S., "Optimal design of laminated composite circular cylindrical shells subjected to combined loads", *J. of Appl. Mech.*, **55**, PP 136-142(1988).
10. Kardomateas, G. A. and Philobos, M. S., "Buckling of thick orthotropic cylindrical shells under combined external pressure and axial compression", *AIAA Journal*, **33**(10), PP 1946-1953(1995).
11. Shen, H. S., "Post-buckling analysis of imperfect stiffened laminated cylindrical shells under combined external pressure and axial compression", *Comput. & Struct.*, **2**, PP 335-348(1997).
12. Xiao, W. and Cheng, S., "Buckling of locally loaded isotropic, orthotropic, and composite cylindrical shells", *J. of Appl. Mech.*, **55**, PP 425-429(1998).

13. Chiba, M., Yamashida, T. and Yamauchi, M., "Buckling of circular cylindrical shells partially subjected to external liquid pressure", *Thin-Walled Structures*, **8**, PP 217-233(1989).
14. Greenberg, J. B. and Stavsky, Y., "Buckling of composite orthotropic cylindrical shells under non-uniform axial loads", *Compos. Struct.*, **30**, PP 399-406(1995).
15. Jones, R. M., "Mechanics of composite material", Hemisphere, Washington, D. C., (1975).
16. Schweizerhof, K. and Ramm, E., "Displacement dependent pressure load in non-linear finite element analysis", *Comput. & Struct.*, **18**(6), PP 1099-1114(1984).
17. Bonet, J. and Wood, R. D., "Non-linear continuum mechanics for finite element analysis", Cambridge University Press, Cambridge, UK, (1997).
18. Crisfield, M. A., "Non-linear finite element analysis of solid and structures", John Wiley, Chichester, Sussex, **1**, (1991).